Lamellar phases and disordered phases of fluid bilayer membranes

1992 J. Phys.: Condens. Matter 4 8649

(http://iopscience.iop.org/0953-8984/4/45/002)

J. Phys.: Condens. Matter 4 (1992) 8649–8670. Printed in the UK

REVIEW ARTICLE

Lamellar phases and disordered phases of fluid bilayer membranes

G Porte

Groupe de Dynamique des Phases Condensées (CNRS—UA 233) and GDR 'Films Moléculaires Flexibles', USTL—Case 026, 34095 Montpellier Cédex 05, France

Received 19 June 1992, in final form 27 July 1992

Abstract. Statistical ensembles of random geometrical shapes pervade complex fluid physics. Initially one-dimensional curves in space were most thoroughly studied due to the many applications of such ensembles to the conformation and dynamics of polymers. But today, ensembles of two-dimensional membranes also attract much attention. Physical realizations of such surfaces include surfactant bilayers which spontaneously self assemble from amphiphilic molecules in solution. At the present time, two different dilute phases of fluid membranes have been well characterized which correspond to different large scale arrangements for the surfaces: the swollen lamellar phase (L_α) and the sponge phase (L_3). In this brief review, we sum up what is understood at the present time of these phases of surfaces. The role of the bending elasticity of the membrane in the phase stability is particularly emphasized.

1. Introduction

In aqueous surfactant solutions, the amphiphilic molecules self-assemble reversibly into a variety of spatially organized structures. These include various mesophases (in concentrated samples) and their disordered analogues. Under appropriate conditions (geometry of the amphiphilic molecules, salinity of the aqueous solvent, ...), there is a preference for sheet-like bidimensional assemblies: it is well known that the smectic lamellar phase occupies a large central area in the phase diagram of most amphiphilic systems.

In the early 1960s, Ekwall *et al* [1] noticed that, for several ternary systems (ionic surfactant/short-chain aliphatic alcohols/water), the domain of stability of the lamellar phase extends very far towards the water corner of the phase diagram. At that time, however, no scattering technique capable of investigating structures of very large spatial periodicity was available and this crucial observation had to be kept on one side.

Later on, numerous observations ([2] and references therein) similar to those of Ekwall were reported for a large variety of amphiphilic systems, ranging from the simplest binary non-ionic surfactant solutions to the most complex systems involving five components: surfactant, cosurfactant, water, salt and oil. Besides the dilute lamellar smectic phase L_α, the so-called anomalous isotropic phase L_3 was soon suspected to be a dilute phase of fluid bilayers as well, but with a different large-scale arrangement. In the meantime, small-angle neutron scattering and high-resolution

0953-8984/92/458649+22$07.50

x-ray scattering were introduced and the structure of L_α and L_3 could thus be investigated in detail. L_α was then proved to consist, as expected, of a regular stack of parallel bilayers with a periodicity d increasing with dilution. On the other hand, the structure of L_3 revealed no long-range order, the bilayers being multiconnected over macroscopic distances along the three directions of space (see figure 1(*c*)). Based on reliable characterizations of structures, our understanding of these phases has deepened quickly in recent years.

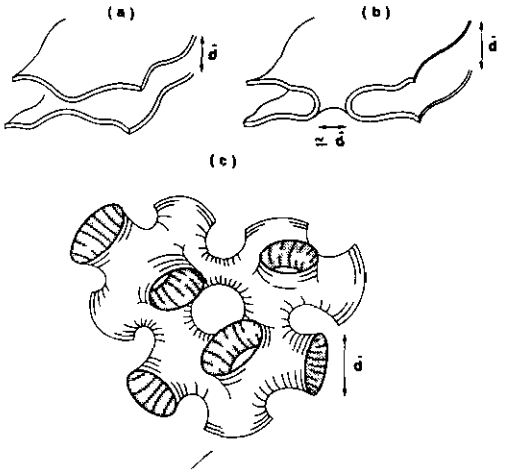

Figure 1. (*a*) Two nearby bilayers in the L_α phase; (*b*) the formation of one elementary 'passage'; (*c*) a schematic picture of the L_3 structure.

As a matter of fact, the experimental evidence for phases of fluid amphiphilic bilayers being stable in the dilute range truly opened up a new field in the physics of complex fluids. At high dilution, the average distance between the membranes is large compared with their thickness and the range of direct molecular interactions. In this limit, they can be considered as being subjected to only one constraint of non-intersection. Since the total area of membrane in the sample is fixed by the total amount of amphiphiles in the phase, but not by any external constraint, the surface tension of the bilayer is vanishingly small. On the other hand, since the amphiphiles prefer to lie in a locally bilayered structure, there will be a substantial excess energy to be spent at the edge if one tries to increase the size of an initially microscopic hole in the membrane. The bilayer may therefore be considered as free of edges and seams (a similar argument indeed working symmetrically for the case of seams). A degree of freedom remains, however, for the membrane to bend into various configurations allowed by the constraint of non-intersection and by the limited volume of the sample where it lives. In this frame, the bending elasticity of the bilayer is the only relevant energetic quantity that weights the probability of one allowed bent conformation versus the others. So, according to these features, we are naturally driven towards especially interesting theoretical objects in statistical physics: random surfaces, for which dilute phases of fluid membranes in amphiphilic systems provide a perfect experimental realization [3]. Although the statistical problem is so expressed in a particularly simple and unambiguous way, its resolution in complete generality is actually a tremendous task that seems currently totally unattainable: the basic difficulty arises from the fact that the topology of the surface is not fixed *a priori*. Therefore, our present understanding was obtained instead from alternate and intricate progresses in experimental observations and in theoretical considerations.

The outline of this short review actually reflects the intricacy involved. In section 2, we recall the unique features of the bending elasticity of bidimensional fluid films versus that of unidimensional threads. In section 3, we summarize the experimental characterization of L_α and L_3 and discuss their relative stability in the light of the membrane elasticity. The random surface model for L_3 is briefly described in section 4. The remarkable scale-invariance is presented in section 5. In sections 6 and 7 two important issues are presented, respectively associated with L_α and L_3: the so-called Helfrich steric interaction in L_α and the hidden symmetry in L_3. Section 8 draws conclusions by summing up the open issues.

2. Bending elasticity of fluid films

The bending elasticity of a bidimensional sheet, fluid within its surface, shows some unique features compared with that of unidimensional flexible thread.

For a thin thread with isotropic cross section, the elastic energy spent upon bending takes the form:

$$\mathrm{d}E = \tfrac{1}{2}Kc^2\,\mathrm{d}l \tag{1}$$

where c is the local curvature imposed on the length element $\mathrm{d}l$. Only one bending modulus K has to be introduced, having the dimension of energy times length. A natural scale length, therefore, immediately comes to mind at a finite temperature T:

$$\langle l\rangle = K/k_\mathrm{B}T \tag{2}$$

which is the well known persistence length [4]; it separates the short scales at which the thread is stiff from the long scales at which the thread essentially behaves as a random walk.

In the case of a bidimensional film isotropic within its surface, the most general expression for the elastic energy has been derived by Helfrich and has the form [5]:

$$\mathrm{d}E = \left[\tfrac{1}{2}K(c_1 + c_2 - c_0)^2 + \overline{K}c_1c_2\right]\mathrm{d}A \tag{3}$$

where c_1 and c_2 are the two principal curvatures and $\mathrm{d}A$ the area element. Three quantities are therefore required to characterize the elasticity: K the mean curvature modulus, $\overline{K}$ the gaussian curvature modulus, and c_0 the spontaneous curvature of the film.

Note, however, that bilayers are built up with two identical monolayers fixed opposite to each other and that the solvent is identical on both sides. Hence, bilayers are locally symmetrical with respect to their midsurface. The energy spent upon bending must therefore be invariant upon changing the signs of both c_1 and c_2, then c_0 vanishes identically. Expression (3) for the bending elasticity of symmetric bilayers then reduces to:

$$\mathrm{d}E = \left[\tfrac{1}{2}K(c_1 + c_2)^2 + \overline{K}c_1c_2\right]\mathrm{d}A. \tag{3'}$$

On the other hand, since K and $\overline{K}$ have the dimension of energy, there is no immediate feeling for a persistence length: this is an important difference from the unidimensional case.

Actually, K and $\overline{K}$ play very different roles [6]. K is related to the energy spent for a locally cylindrical deformation of the surface: it is therefore involved in any sinusoidal wave-like curvature mode of the surface. So its effect on the bending statistics of the surface is to control the average square amplitude of the thermal bending modes (just like the rigidity modulus for thin thread). On the other hand, the role of $\overline{K}$ has no unidimensional counterpart. Let us recall the Gauss–Bonnet theorem, which states that the integral of the gaussian curvature over a given surface with no edges is a topological invariant. More precisely, we have:

$$\int_A c_1 c_2 \, \mathrm{d}A = 4\pi(n_p - n_h) \tag{4}$$

where n_p is the number of disconnected parts of the total surface A and n_h is the number of 'connections' or 'handles' of the surface. Therefore, it is clear in (3′) that $\overline{K}$ works as the chemical potential for the degree of connectivity of the structure. Strongly negative values of $\overline{K}$ favour the formation of many disconnected pieces with no rims, like spherical vesicles, while positive values will favour the formation of one large aggregate, preferably having a multiconnected structure (high 'genus' surface, see figure 1(*c*)). Then $\overline{K}$ plays its role each time a structural transformation involves a topological change for the membranes. On the other hand, $\overline{K}$ has no effect as long as curvature fluctuations take place at constant topology or degree of connection. In this latter case, only K is involved.

3. Structures and phase behaviour

At the present time, two dilute phases of fluid membranes have been well characterized: the swollen lamellar phase L_α and the so-called anomalous isotropic phase L_3 (or sponge phase). Both phases have been shown to consist of infinite (or almost) membranes, but with very different large-scale average arrangements. The structure of L_α is simpler to describe ([7] and references therein; [8–11]). Its texture in polarized microscopy shows focal conics and oily streaks which are the unambiguous signature of a quasi-long-range smectic order. Further investigations using x-rays or neutron scattering reveal the correlative existence of a Bragg peak (see figure 2), the position of which is consistent with the idea of parallel bilayers, regularly stacked normal to the direction of the director of the phase. In these respects, the swollen L_α phase is nothing different from the classical lamellar phase usually found in the concentrated part of the phase diagram. However, the intriguing fact here is the persistence of the long-range smectic order at high dilution, in spite of its very large periodicity compared with the range of direct molecular interactions.

In contrast, the optical observations and the scattering patterns in the L_3 samples reveal neither orientational nor positional long-range order. The structure is less easy to visualize and, so far, has not been proved unambiguously. However, extensive experimental investigations combining x-rays and neutron scattering data, together with measurements of transport properties [12–15] (conductivity and self-diffusion of the components) strongly suggest a structure similar to the picture drawn schematically in figure 1(*c*). This picture was further supported later on by freeze-fracture electron microscopy [16]. It is easier to visualize the main features of this structure following the steps shown in figure 1. Starting from L_α, it is easy to imagine

the formation of one individual connection by local fusion of two adjacent bilayers. Doing so we induce one elementary change of the topology of L_α. Spontaneous proliferations of such 'connections' on both sides of each membrane will, as a first effect, kill the smectic order of the initial lamellar phase at some stage, and then ultimately result in the formation of the structure drawn in figure 1(*c*) which, we think, appropriately represents the basic features of the L_3 structure. These features are as follows:

(i) the structure is isotropic with no long-range positional order;

(ii) the bilayer is bent almost everywhere, with its principal curvatures of opposite sign (saddle-like local shape), so that it is, on a large scale, multiconnected to itself in the three directions of space;

(iii) as the membrane is intrinsically symmetrical with respect to its midsurface, we expect it to divide space in two, on average, equivalent subvolumes in most cases (this symmetry may be broken in some cases, as will be discussed in section 7;

(iv) in spite of the absence of long-range order, the scattering pattern (x-rays or neutron, see figure 3) clearly shows a well defined maximum, corresponding to a structural length which we identify with the average diameter of the 'connections' or 'passages'.

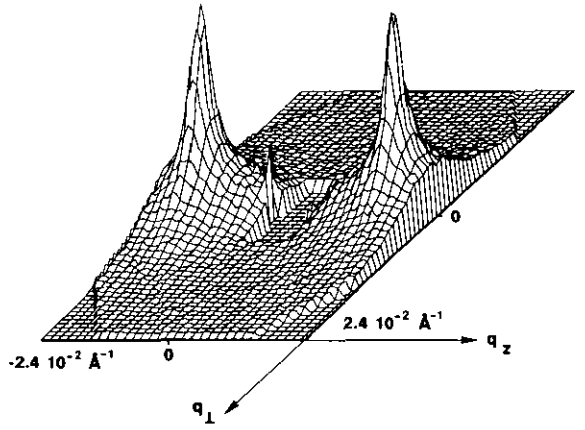

Figure 2. A typical scattering pattern of a L_α swollen sample exhibiting Bragg singularity. System: CPCl/n-hexanol/brine; $\bar{d} = 360$ Å, $\phi = 0.094$.

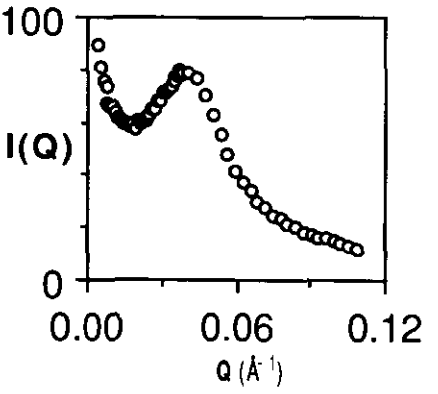

Figure 3. A typical scattering pattern of an L_3 sample. There is no Bragg singularity, but still one notes a broad correlation maximum. System: CPCl/n-hexanol/brine: $\bar{d} = 160$ Å, $\phi = 0.187$.

There is *a priori* no reason for the structures of L_α and L_3, as shown in figure 1, not to be decorated by small disconnected subunits (such as vesicles, tori or more complicated bretzels) of size smaller than $\bar{d}$. Note, however, that the excess mean curvature elastic energy involved in such disconnected subunits is at least of the order of $8\pi K$. Therefore, a noticeable proportion of disconnected objects will not be observed unless $\overline{K}$ is sufficiently negative, so that this excess mean contribution is compensated by the gaussian contribution. As a matter of fact, the scaling behaviour described in section 5 indicates that the relative amount of membrane in disconnected pieces is very small.

Since the pioneering observations of Ekwall *etal*, L_α and L_3 have been observed in a large number of systems. These include the most simple binary systems such as $C_{12}E_5$/water [15]. In this case, the phase diagram is truly bidimensional (we neglect pressure as a rather irrelevant field variable) and is usually drawn versus the two variables ϕ, the volume fraction of amphiphile, and T, the temperature. For systems involving more than two components (such as the quaternary systems ionic surfactant/short-chain alcohol/water/salt) the complete phase behaviour needs to be represented in a space of higher dimensionality. However, it is possible to represent any two-dimensional sections of the diagram. Appropriate choices for the section actually reveal a strikingly similar geometry for the phase behaviour. For the quaternary systems for instance [17], we may choose to fix T and the salinity of the brine, letting free ϕ and the alcohol-to-surfactant ratio or alternately fix T and the alcohol-to-surfactant ratio and let free ϕ and the salinity. Doing so, we fix either the properties of the solvent or the chemical composition of the aggregates. Plotting the phase behaviour as a function of ϕ and the remaining free parameter, which we generically denote from now on as χ (figure 4(*c*)), we find a quite remarkable geometry in the dilute range. Usually, three phases are seen in this range, depending on χ. For low χ-values, L_1 takes place, which consists of globular or unidimensional micelles. These structures are beyond our present scope and we shall not discuss them here. L_α and L_3 take place successively as χ increases. Their phase boundaries are roughly horizontal in a moderate concentration range, which means that their stability is rather independent of the degree of dilution ϕ. Only in the very dilute range can we see strong deviations from horizontality for the phase boundaries.

In order to interpret the relative positions of the L_α and L_3 domains versus χ, we turn back to expression (3′) for the bending elasticity of the membranes. A most striking difference between the two structures is certainly the difference in topology. In the lamellar phase, each presumably infinite bilayer is singly connected to itself over its whole area. In contrast, the bilayer in L_3 is multiply connected to itself in the three directions of space. So $\overline{K}$ is here certainly involved. We expect that smaller (possibly negative) values of $\overline{K}$ will rather favour L_α and, conversely, for higher (possibly positive) values we rather expect the multiconnected topology of L_3. To investigate this point more deeply, let us remind ourselves that a bilayer consists basically of two amphiphilic monolayers fixed opposite to each other in a symmetrical structure. In contrast with the bilayer, each monolayer is not in itself a symmetrical film and its spontaneous curvature $c_{0,\mathrm{mono}}$ is, but exceptionally, not zero. Hence, when fixed to each other in a planar bilayer, each monolayer will feel frustrated [3]. A possibility, to partially release the frustration, is to allow deviations from the planar conformation of the bilayer. When $c_{0,\mathrm{mono}}$ is negative (i.e. with concavity towards the solvent, figure 5(*a*)), a more favourable conformation for the bilayer is actually a saddle [18, 19]. At the level of the midsurface, the mean curvature $(c_1 + c_2)$ is still zero. But considering the mean curvatures of the monolayers at the level of their surfaces of inextension (obtained by parallel displacement from the midsurface at distances $\pm\epsilon$ where ϵ is of the order of $\delta/2$), one immediately sees that they have identical finite magnitudes and symmetrically negative signs (and are therefore closer to the negative values of c_0). This intuitive picture can be further formalized starting from the bending elasticity of the monolayer:

$$\mathrm{d}E_{\mathrm{el,mono}} = [\tfrac{1}{2}K_{\mathrm{mono}}(c_1 + c_2 - c_0)^2 + \overline{K}_{\mathrm{mono}}c_1c_2]\,\mathrm{d}A \tag{5}$$

from which the elasticity of the bilayer can be derived easily provided that we assume

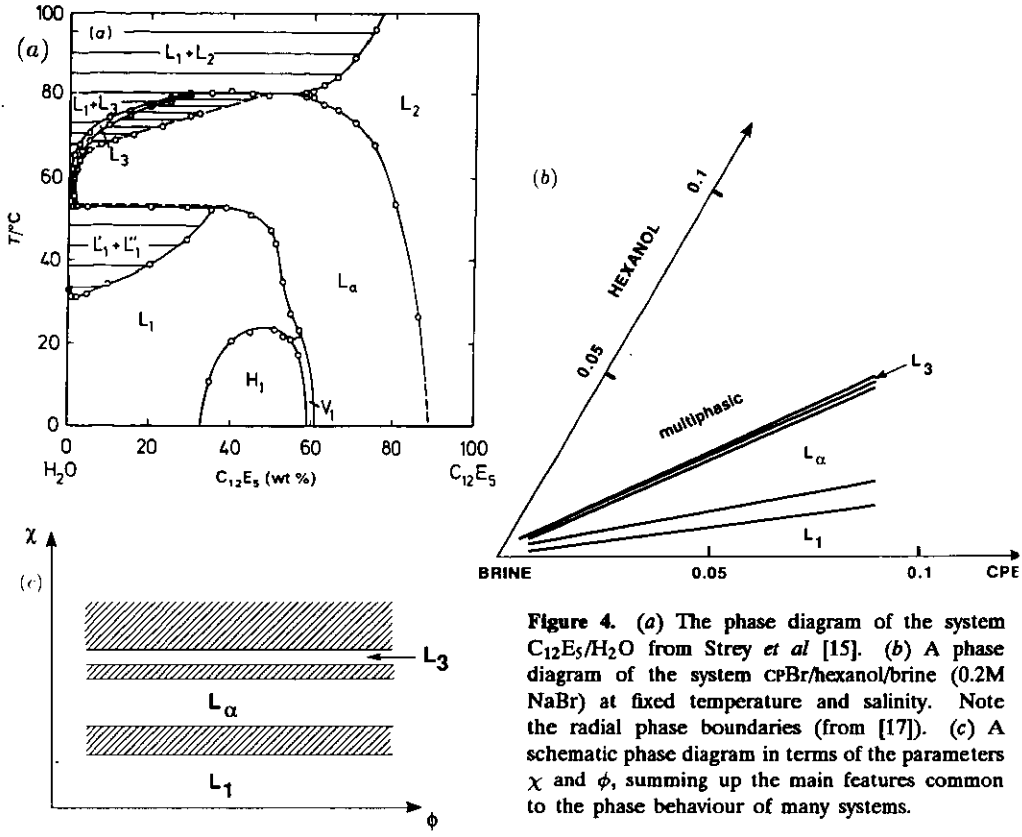

Figure 4. (*a*) The phase diagram of the system $C_{12}E_5/H_2O$ from Strey *et al* [15]. (*b*) A phase diagram of the system CPBr/hexanol/brine (0.2M NaBr) at fixed temperature and salinity. Note the radial phase boundaries (from [17]). (*c*) A schematic phase diagram in terms of the parameters χ and ϕ, summing up the main features common to the phase behaviour of many systems.

that the surfaces of inextension of the monolayers remain at a constant distance $\epsilon/2$ from the midsurface. We thus obtain [14]:

$$\begin{aligned} c_{0,\mathrm{bil}} &= 0 \\ K_{\mathrm{bil}} &= 2K_{\mathrm{mono}} \\ \overline{K}_{\mathrm{bil}} &= (2\overline{K}_{\mathrm{mono}} - 4\epsilon c_0 K_{\mathrm{mono}}). \end{aligned} \tag{6}$$

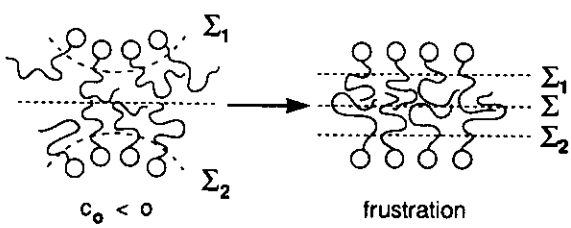

Figure 5. (*a*) Two monolayers with negative spontaneous curvature c_0. (*b*) When fixed opposite to each other they 'feel frustrated'. Note that Σ_1 and Σ_2 represent the respective surfaces of inextension.

It is clear in (6) that negative values of c_0 bring a positive contribution to $\overline{K}_{bil}$, making the formation of a saddle easier (or equivalently making the formation of multiconnected structures such as L_3 easier). It is interesting, in this picture, to note that for all systems the generic parameter χ is known to induce a monotonic decrease of c_0. In the case of a binary system with non-ionic surfactants it is known that the affinity of polyoxyethylene groups for water decreases upon increasing T: the polar groups expel bound water molecules, come closer to each other at constant tail volume and hence decrease c_0. Similarly, in quaternary systems it has been proved in [20] that increasing the relative amount of alcohol in the monolayer actually decreases c_0. Also, increasing salinities screen better and improve the electrostatic repulsions between the ionic head group; this allows a closer packing of the head groups and the higher salinity ultimately decreases c_0.

Thus, these considerations of c_0 and $\overline{K}_{bil}$ actually make sense of the relative positions of L_α and L_3, while increasing the generic parameter χ. However, they focus on the topology and forget fluctuations. If these fluctuations were to be neglected, the two phases should be in their ground state (figure 6): L_α would consist of perfectly flat bilayers and L_3 would have the structure of one of the many 'periodic minimal surfaces' currently known. For these two perfectly ordered structures, the mean curvature is zero everywhere, so that the difference in elastic energy between them only arises from the gaussian term in (3'): the structural transformation takes place for $\overline{K}$ being exactly zero. Several facts actually indicate that neglecting fluctuations is not permitted here. First, L_3 is clearly not long-range ordered. Also, in the ground-state picture, the range of stability of the L_3 structure should have zero thickness in the χ- (or $\overline{K}$-) direction. As soon as $\overline{K}$ increases beyond zero, where L_α becomes unstable, there is a constant gain of elastic energy in increasing the connectivity of the membrane with no limits and the L_3 structure should immediately collapse up to the point where anharmonic terms in the elastic energy come into play (high concentration). The existence of dilute L_3 structures implies that some entropic contribution dampens the abruptness of the structural transformation here and somehow prevents the collapse over a finite $\overline{K}$ range. This entropic contribution, we guess arises from curvature fluctuations. Lastly, as we shall see in a later section, the persistence of smectic order in L_α at high dilution can be understood in terms of the so-called steric interaction between parallel membranes. Actually, this effective interaction arises from the interplay between the constraint of non-intersection and the spontaneous curvature fluctuations of the membranes. Thus, fluctuations have to play a crucial role in the phase behaviour.

Unfortunately, evaluating the fluctuations is actually a very difficult issue. Things are not so bad for the L_α phase where the existence of smectic order makes it possible to expand any given configuration into classical normal modes [21]. The difficulty arises with the L_3 phase where the liquid structure makes such a procedure impossible. Hence, more approximate approaches are to be used: the random surface model presented in the following section is such an attempt.

4. The random surface model for L_3

This model for the structure of L_3 was first proposed by Cates *et al* [22] and, later on, a more refined version was reported by Golubovic and Lubensky [23]. The primary aim here is quite the opposite to that of the preceding section: to focus on the

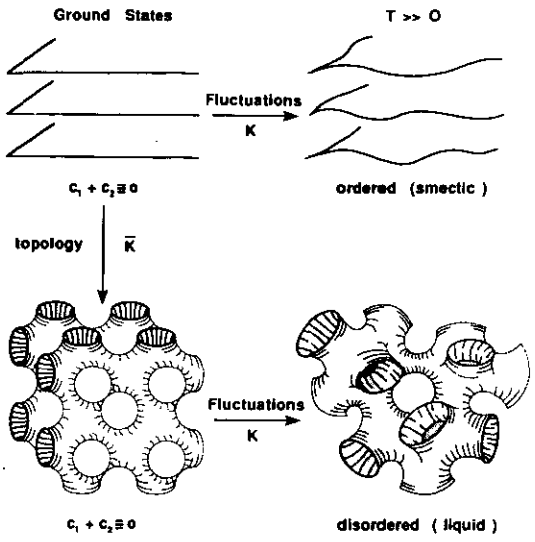

Figure 6. A schematic representation of L_α and L_3 with their 'ground-state' analogues illustrating the roles of K and $\bar{K}$ in their relative stabilities.

fluctuations and neglect the topology, i.e. emphasize the role of K, forgetting that of $\bar{K}$. For the sake of simplicity $\bar{K}$ is therefore set to zero. The space is then coarse-grained using a cubic lattice of cell size ξ (where ξ is essentially of the order of the characteristic distance $\bar{d}$ exhibited by the scattering patterns of L_α and L_3). The cells of the lattice are randomly labelled A and B with respective probabilities Ψ and $1-\Psi$ where Ψ is not determined *a priori* but rather used as a variational parameter. The surface (i.e. bilayer) is then forced to lie at the interface between A and B domains. One thus obtains a highly randomized model of a non-intersecting surface with no edges and seams. It is here assumed to give an appropriate representation of the L_3 disorder. The entropy density of L_3 is then simply that of the random mixing of labels A and B. It has the well known form

$$S = -(k_B/\xi^3)[\Psi \ln \Psi + (1-\Psi)\ln(1-\Psi)] \tag{7}$$

and the bending-energy density is heuristically estimated:

$$F_{\text{bend}} = (1/\xi^3)8\pi\Psi(1-\Psi)K. \tag{8}$$

For the sake of comparison of phase stabilities, it is necessary to estimate the free-energy density of L_α for which the coarse-graining procedure is not appropriate. Thus, the authors adopted the well known expression derived by Helfrich (see section 6):

$$F_{L_\alpha} = (3\pi^2/128)(\phi/\delta)(k_B T)^2/K\bar{d}^2 \tag{9}$$

where $\bar{d} = a(1-\phi)/\phi$ denotes the interlamellar spacing and a the thickness of the membrane.

From these expressions for the free-energy densities, the phase behaviour was computed numerically as a function of the reduced mean curvature rigidity K/T.

The important predictions of the model are as follows.

(i) At high K/T, the L_α phase is stable. Upon lowering K/T, the $L_\alpha \rightarrow L_3$ transition takes place when, roughly speaking, the mean curvature energy spent becomes less than the entropy gained in melting the positional and orientational order of the smectic L_α structure. The L_3 phase obtained is then symmetrical with respect to the Ψ parameter ($\Psi = 1 - \Psi = \frac{1}{2}$).

(ii) Upon further lowering of K/T, the model explicitly produces a spontaneous breaking of the Ψ symmetry of L_3. This more important issue is discussed in section 7.

Some questions about this model must, however, be further discussed. The first question concerns the coarse-graining procedure. Similar coarse-graining procedures are indeed used in the lattice gas models, which proved to be relevant for the statistics of random polymers. In these cases, however, the cell size of the lattice is indeed related to the natural length of the problem—the persistence length—but certainly *not* to the concentration in polymers. In the present case, we mentioned that no natural length characteristic of the membrane could be inferred immediately. And the question arises of what length ξ to use for the cell size of the coarse-grained space? Cates *et al* [22] chose ξ to be determined by the area density of membrane per unit volume of the sample. This choice was justified by the experimental fact that the structural length $\bar{d}$, as evidenced from the scattering patterns of L_α and L_3, actually shows a simple swelling behaviour upon dilution ($\bar{d} \sim \phi^{-1}$). We shall make sense of this remarkable property in the next section which deals with the scale-invariance of the statistics of fluid membranes.

An important reservation about this model must be underlined, however. The random-mixing assumption implies that all different labellings of nearby cells have the same probabilities. Hence, one particular labelling giving to the surface the form of the coarse-grained analogue of a hemispherical cup locally must involve the same elastic energy as one leading to the formation of a local saddle (figure 7). This implies explicitly that $\bar{K} = -K$ (rather than $\bar{K} = 0$, as initially proposed by the authors of [22, 23]) so that the elastic energy is of the form:

$$\mathrm{d}E_{\mathrm{el}} = \tfrac{1}{2}K(c_1^2 + c_2^2)\mathrm{d}A \tag{10}$$

where the relative signs of c_1 and c_2 are irrelevant. Any significant departure from this specific situation not only affects the heuristic expression of F_{bend} (8) (which could presumably be improved by the addition of a $\bar{K}$-dependent contribution), it also makes the random-mixing assumption less and less justified [14] since saddles (or conversely hemispheres) will be favoured against hemispheres (conversely saddles), thus inducing stronger and stronger correlations between nearby cells.

Nevertheless, from this section and the preceding one, we understand, at least qualitatively, the roles of the two rigidities K and $\bar{K}$ in the phase stability. $\bar{K}$ is involved due to the change of topology and is controlled by the experimentally tunable parameter χ via c_0, the spontaneous curvature of the amphiphilic monolayer. K controls the amplitude of the fluctuations and, in this respect, is presumably involved in the offset of smectic order when the L_α-to-L_3 transition takes place.

5. Scale-invariance

As underlined in the previous sections, the rationalization of the phase behaviour in terms of membrane elasticity remains rough and qualitative due to the extreme

difficulty of a fully consistent computation of the free energy of the disordered structure of L_3. There is a point, however, where more quantitative predictions can be made: the evolution of the free energies as a function of dilution.

These scaling laws are actually consequences of the unique feature of the membrane-bending elasticity, already underlined in section 2: the reduced rigidity moduli K/k_BT and $\overline{K}/k_BT$ are pure numbers. This means that the elastic energy in (3′) is invariant with respect to any isotropic dilation. A dilation of ratio λ changes c_1 and c_2 into c_1/λ and c_2/λ and dA into $\lambda^2 dA$ so that dE_{el} remains invariant.

Let us consider two systems [14] (figure 8) involving respective total areas of membrane A and $A' = \lambda^2 A$, confined in respective volumes V and $V' = \lambda^3 V$. Note that for both L_α and L_3 structures, the ratio V/A (respectively V'/A') can be identified essentially with the characteristic distance $\overline{d}(\overline{d}')$ up to some geometrical prefactor of order unity. However, the argument is general enough to be applied even in the case of a structure exhibiting no well defined characteristic distance. Thus, we work it out keeping A and V (rather than A and $\overline{d}$) as the parameters defining the considered situation. Apart from the small thermal ripples of wavelength smaller than $\overline{d}$ and $\overline{d}'$, any configuration of the first system corresponds to a dual configuration of the second system through the isotropic dilation of ratio λ. These dual configurations, having the same elastic energy, have identical statistical weights and therefore bring the same contribution to the free energy of each system. This means that the contribution of the large-scale (i.e. excepting the small ripples) configurations of the membranes to the free energy is scale-invariant just like the bending elastic energy. Since this contribution must also be extensive it necessarily scales as A^3/V^2. The next step is to include the contribution of the thermal small ripples. In the rigid limit ($K/T \gg 1$) these modes are independent, so that their contribution to the free energy is simply proportional to A (or $A' = \lambda^2 A$). Putting together the two contributions, we arrive at the free energy of the necessary form

$$F = \mu_A A + B_A(K, \overline{K}, T) A^3/V^2 \tag{11}$$

A/V being proportional to ϕ ($\phi = \delta A/V$), equation (11) can be immediately translated in terms of the free-energy density:

$$f = F/V = \mu_\phi \phi + B_\phi(K, \overline{K}, T)\phi^3 \tag{12}$$

where $B_\phi(K, \overline{K}, T)$ is an unknown function of K, $\overline{K}$ and T. We can go one step further, noting that K and $\overline{K}$ are involved in the partition function only in their reduced form: K/T and $\overline{K}/T$. Hence, $B_\phi(K, \overline{K}, T)$ necessarily has the form $T/\beta(K/T, \overline{K}/T)$. Thus, finally, the free-energy density of dilute phases of fluid membranes should have the form

$$f = F/V = \mu_\phi \phi + T\beta(K/T, \overline{K}/T)\phi^3. \tag{13}$$

The first term in (13), linear in ϕ, is trivial and does not affect the stability and the physical properties of the phases. The second term, which scales as ϕ^3, expresses the scale-invariance of the statistics of membranes and therefore plays the central role.

Two basic conditions, necessary for the scale-invariance to apply, must be underlined. The first one is that the phase consists of infinite membranes only: a

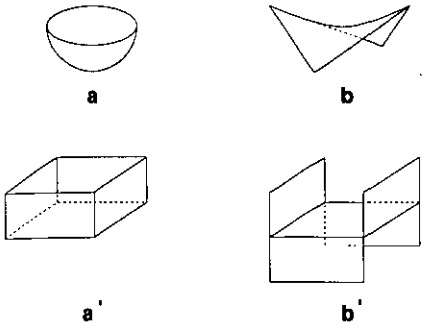

Figure 7. Hemispherical cups and saddles and their coarse-grained analogue in the model of section 4.

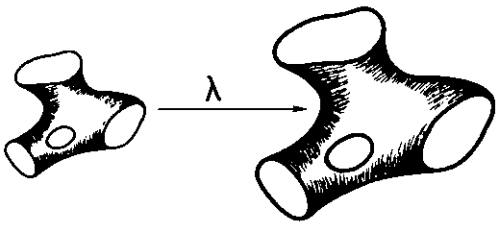

Figure 8. Scale-invariance: the 1-system and λ-system.

substantial proportion of disconnected subunits will bring in the contribution of their entropy of dispersion, which is indeed not scale-invariant. Secondly, the interactions between membranes must be restricted to the constraint of non-intersection: any molecular force having a finite range comparable to $\bar{d}$ will introduce a scale-dependent contribution into the membrane's Hamiltonian and, therefore, break the scale-invariance. These conditions are actually obeyed for L_α and L_3, at least in the moderate dilution range [24].

The consequences of scale-invariance are of crucial importance. It implies that dilution acts on the structure of a given phase as a simple dilation, any average characteristics length being simply proportional to the inverse volume fraction of membranes, i.e. $\bar{d} \sim \phi^{-1}$. The scattering patterns of one given phase at different concentrations along a dilution line (constant K/T and $\bar{K}/T$) should remain identical when plotted as a function of the reduced wave vector $Q = q\bar{d}$ (i.e., q/ϕ) [25]. A convincing experimental illustration of this expectation is shown in figure 9. This also means that if one given phase is found stable at one given concentration it remains stable all along the corresponding dilution line; so no phase transition is expected upon variation of ϕ alone. The horizontality of the phase boundaries observed in the moderate concentration range (see section 3) appears here as a direct consequence of the scale-invariance of the membranes statistics.

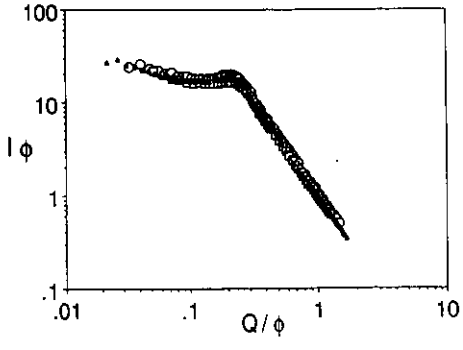

Figure 9. Scattering patterns of L_3 at various dilutions in reduced units. System: AOT/brine (from [25]).

Moreover, expression (13) for the free-energy density can be used to derive scaling laws for other measurable physical properties of phases of fluid membranes [24]. For

instance, the osmotic compressibility of the isotropic phase (L_3) can be obtained via a suitable differentiation of F/V:

$$\pi = -f + \phi \partial f / \partial \phi \sim \phi^3 \tag{14}$$

so that the intensity scattered at zero wave vector is

$$I(0) = \phi(\partial \pi / \partial \phi)^{-1} \sim \phi^{-1}. \tag{15}$$

However, an important prerequisite for (13) to be valid is that the small thermal ripples can be analysed as combinations of independent normal modes, that is true only in the rigid limit ($K/T \gg 1$). Only in this limit can the increase of area compared with its projected value be neglected and the dilution be identified with a pure dilation. Perturbation calculations worked out recently have shown that the effect of small wavelengths' curvature fluctuations is to renormalize the effective values of A, K and $\overline{K}$. Up to the first order in T/K, the following expressions have been obtained for the renormalized quantities [26–28]:

$$A(\xi) = A_0[1 - (k_B T/4\pi K_0) \ln(\xi/a)] \tag{16}$$

$$K(\xi) = K - (3k_B T/4\pi) \ln(\xi/a) \tag{17}$$

$$\overline{K}(\xi) = \overline{K}_0 + (10k_B T/12\pi) \ln(\xi/a) \tag{18}$$

where the subscript 0 stands for the true bare values, $A(\xi)$ is the effective (or projected) value of the area of membrane and $K(\xi)$ and $\overline{K}(\xi)$ the effective rigidities. a is the short-wavelength molecular cut-off and ξ is the scale length at which the effective values are involved. For L_α and L_3, the relevant scale length ξ is indeed of the order of $\overline{d}$, the characteristic structural length.

As a first consequence, the renormalizations actually break up (to some extent) the scale-invariance, since each change in scale implies a redefinition of the membranes' characteristics. However, the variations of the effective A, K and $\overline{K}$ are logarithmic in ξ (i.e., $\overline{d}$ or ϕ) and hence very slow. As discussed in [29], expression (13) for the free-energy density has to be corrected accordingly. It should still exhibit a main ϕ^3-dependence but be modified by a factor of order $\ln \phi$, and we expect rather

$$f = F/V \sim \phi^3(1 + c \ln \phi). \tag{19}$$

Similarly, expression (15) for the ϕ-dependence of osmotic compressibility has to be modified. Differentiation of (19) immediately gives

$$I(0) = \phi(\partial \pi / \partial \phi)^{-1} \sim [\phi \ln(\phi/\phi^*)]^1 \tag{20}$$

an expectation that can be checked experimentally using light scattering [29] (an example is shown in figure 10).

More dramatic consequences of the renormalizations are further expected at extreme dilutions. At some stage the scale ξ (i.e., $\overline{d}$) becomes so large that the correction term in the expression of the effective rigidity $K(\xi)$ makes it small compared with $k_B T$. The bending energy of curvature fluctuations of large amplitudes is negligible and we then enter the strong fluctuation regime, where scale-invariance is definitely lost. As mentioned in section 2, no immediate notion of a persistence length

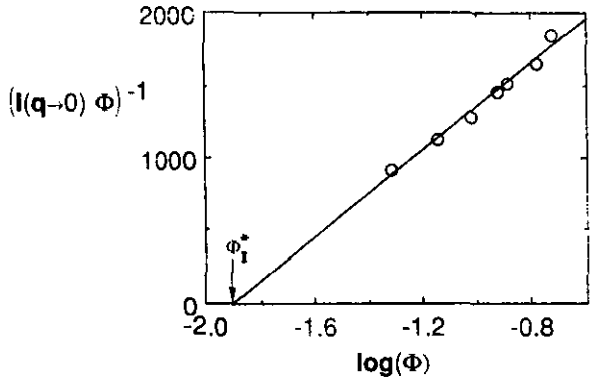

Figure 10. $[\phi I(0)]^{-1}$ versus ln ϕ in the L_3 phase. System: AOT/brine (from [25]).

could be inferred from examination of the bending elasticity of a fluid symmetric bilayer. However, the existence of a persistence length ξ_K is here introduced via renormalization of the effective rigidity $K(\xi)$. Defining ξ_K as the scale beyond which $K(\xi) \simeq 0$, we obtain [30]

$$\xi_K = a \exp(4\pi K_0/3k_B T). \tag{21}$$

We note that, in contrast with the case of 1D threads, ξ_K does not increase linearly with the rigidity, but exponentially.

Putting together the main features reported in this section, we are driven to a quite simple general picture. Starting with a membrane having a bare rigidity K_0, larger than $k_B T$, one distinguishes two dilution ranges.

(i) The moderate dilution range, where K_{eff} is still larger than $k_B T (\bar{d} \ll \xi_K)$. The scale-invariance, weakly broken by logarithmic renormalizations, actually rules the phase behaviour and the physical properties: the phase boundaries are roughly horizontal and the osmotic compressibility scales according to (20).

(ii) At very high dilution ($\bar{d} > \xi_K$), K_{eff} is negligible. The phase boundaries are no longer horizontal, and the scaling laws derived from the perturbation approach are no longer relevant. This regime is totally dominated by the fluctuations.

6. Smectic order in dilute L_α: the steric interaction

An especially intriguing property of the swollen lamellar phase is the persistence of its smectic order at dilutions such that the average intermembrane distance $\bar{d}$ is very large compared with the range of the direct molecular forces between bilayers. Smectic order implies that some long-range effective force is present that strongly correlates the relative positions of adjacent bilayers in the stacking.

The nature of this effective interaction was first understood by Helfrich [21] in terms of the constraint of non-intersection for nearby membranes. Consider one isolated membrane free to fluctuate in 3D space. Due to its thermal curvature fluctuations it scans a very large volume in direct space. When confined in between two hard walls (or two adjacent membranes), a large number of initially allowed

bent conformations is now forbidden by the constraint of non-intersection: the configuration entropy of the membrane is thus decreased by confinement.

The corresponding free-energy variation ΔF is positive, leading to the idea of an effective repulsive steric interaction between membranes. Expressed per unit area of membrane in the lamellar stacking it has the well known form [21]:

$$\Delta F/A = (3\pi^2/128)(k_B T)^2/K\bar{d}^2. \tag{22}$$

This expression was derived by Helfrich, expanding the microstates of smectic stacking into normal modes. A simpler and perhaps more appealing procedure is as follows. First, note that the $\bar{d}^{-2}$-dependence of $\Delta F/A$ simply expresses the scale-invariance described above. Translating expression (13) in terms of the free-energy variation per unit area of membranes, one gets immediately

$$\Delta F/A = T\beta_{L_\alpha}(K/T, \overline{K}/T)\delta^3/\bar{d}^2. \tag{23}$$

(The term linear in ϕ in (13) is dropped here because we now consider the free-energy variation compared with that of the free isolated membrane taken as the reference state.) Since the confinement does not involve topological changes, $\overline{K}$ plays no role and β_{L_α} only depends on K/T. In order to evaluate this dependence, we again use a spatial transformation, but different from that used in section 5. Taking Oz as the direction of the director of the smectic phase (direction of the average normal of the bilayers) and xOy parallel to the average bilayers, we define the transformation T_λ according to:

$$\begin{aligned} x' &= \lambda x \\ y' &= \lambda y \\ z' &= z \end{aligned} \tag{24}$$

which relates the coordinates of the generic point $r(x, y, z)$ to those of its transform $r'(x', y' z') = T_\lambda(r)$, see figure 11. This transformation changes dA into $dA' = \lambda^2 dA$ and each c_1 and c_2 into c_1/λ^2 and c_2/λ^2, but $\bar{d}$ (in the z-direction) remains unchanged. Consider (figure 11) two systems (1-system and λ-system) of the same smectic periodicity $\bar{d}(\bar{d}' = \bar{d})$, containing respective areas of membranes A_1 and $A_\lambda = \lambda^2 A_1$, having respective mean curvature rigidities K_1 and K_λ.

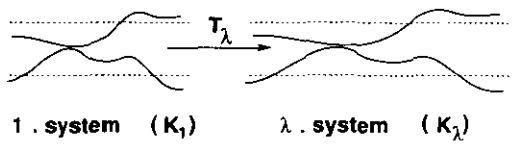

Figure 11. Steric interaction in L_α: a definition of the T_λ spatial transformation.

Forgetting again the small ripples, the transformation T_λ carries in a duality correspondence between all the microstates of the 1-system and all those of the λ-system. Dual microstates have the same elastic energy and hence identical statistical weights only if

$$K_\lambda = \lambda^2 K_1. \tag{25}$$

Provided that condition ΔF_1 and ΔF_λ are identical, we have therefore

$$\Delta F(A, K/T, \bar{d}) = \Delta F(\lambda^2 A, \lambda^2 K/T, \bar{d}). \tag{26}$$

Using (23), we immediately get:

$$\beta(K/T) = \lambda^2 \beta(\lambda^2 K/T) \tag{27}$$

which implies that $\beta(K/T)$ is of the form:

$$\beta(K/T) \sim T/K. \tag{28}$$

Combining (23) and (28), one obtains a scaling law, having a form identical to that of Helfrich (expression (22)):

$$(\Delta F/A)_{L_\alpha} \sim T^2/K\bar{d}^2. \tag{29}$$

However, the counterpart of the simplicity of these scaling arguments is that, in contrast with Helfrich's procedure, we cannot predict the magnitude of the prefactor in expression (22).

Since $(\Delta F/A)_{L_\alpha}$ varies as $\bar{d}^{-2}$, the effective steric interaction between infinite membranes is a long-range force, as required by the existence of smectic order. These ideas can actually be checked against experimental data. The free-energy density can be translated in terms of the smectic compressibility B of the lamellar stacking:

$$B = d^2(\partial^2 f/\partial d^2)_n. \tag{30}$$

The bending rigidity K_S, of smectic stacking, can be expressed immediately as a function of that of the individual membrane:

$$K_S = K/\bar{d}. \tag{31}$$

The smectic elasticity of L_α has the usual form:

$$E = \frac{1}{2}\sum_q (Bq_z^2 + K_S q_\perp^4)|u_q^2| \tag{32}$$

where the u_qs are the Fourier components of the local displacement $u(r)$ and q_z and $q_\perp$ are the coordinates of wave vector q respectively along the z-direction (parallel to the director) and in the xy-plane (normal to the director). As first shown by Caillé [31] the scattering factor of smectic media is singular at the nominal Bragg position $q_0 = 2\pi/\bar{d}$ and has the form of a power law [32]

$$I(0, 0, q_z) \sim (q_z - q_0)^{-(2-\nu)} \tag{33}$$

where the exponent ν is related to B and K_S as follows:

$$\nu = q_0^2 k_B T/8\pi\sqrt{BK_S}. \tag{34}$$

For smectic stacking, where the membrane positions are correlated by pure steric interaction, B is obtained from (30) and (22); and from (34) we get

$$\nu_{st} = 4/3. \tag{35}$$

The exponent ν_{st} of the Bragg singularity (at sufficient dilution) is therefore a pure universal number. This expectation can be checked by quantitative treatments of the scattering pattern of L_α samples at different dilutions and from different systems [9–11]. The data reported in [10] are especially accurate since they are collected using high-resolution x-ray scattering. They were found to be in excellent agreement with Helfrich's expectations: in particular, the measured exponent ν_{st} is found to be close to the predicted value 4/3, indicating that the prefactor $3\pi^2/128$ in the free-energy density (22) as computed by Helfrich is in fact close to reality.

In principle, the scaling law in (22) should be corrected as well for the logarithmic renormalizations of A, K and $\overline{K}$. However, at the present time no measurement of B has been accurate enough to show these deviations. On the other hand, thanks to the existence of a quite sharp peak at q_0 in L_α, one can obtain direct evidence for the renormalization of the area of membrane A. In the case of totally flat bilayers we expect

$$q_0 = 2\pi/d \qquad \phi = \delta/\bar{d}. \tag{36}$$

If the bilayers are submitted to thermal curvature fluctuations, we expect from (16):

$$\phi = \delta A_0/\overline{dA}. \tag{37}$$

Using (16) for the ratio A/A_0 with $\xi = \bar{d}$ and $\phi \sim \bar{d}^{-1}$ one obtains

$$\phi\bar{d} = \delta[\alpha - (k_B T/4\pi K_0)\ln\phi] \tag{38}$$

where α is a constant quite close to 1.

With both ϕ and q_0 being measured accurately, the $\ln\phi$ deviation beyond exact invariance is found to be appreciable [15, 25, 33] (see an example in figure 12). Moreover, the prefactor being proportional to T/K_0, plotting $\phi\bar{d}$ versus $\ln\phi$ provides a quite simple way to estimate K_0 once the thickness δ of the membrane is known from some other experimental data [34]. K_0 for the bilayers in the L_α phase of several systems has been measured according to this procedure. As a matter of fact, all K_0s are found close to $k_B T$ (from $0.6k_B T$ to $4k_B T$). This finding is probably related to the fact that the steric interaction decreases when K_0 increases (K_0^{-1}-dependence): if the membranes are too rigid, the steric interaction is not strong enough to overcome the van der Waals' attractions and the lamellar phase does not swell upon dilution.

7. Symmetry in the L_3 phase

Actually, the free-energy cost to make small loops of defects such as rims or seams in the membrane is finite. These defects are therefore certainly present in any macroscopic volume of L_α or L_3. However, as long as their free energy per unit

length is large enough their number density and average size remain small. In this limit, their presence will alter the properties of the phase only locally, and it is instructive to consider the simplified picture where they are omitted. The meaning of the symmetry of L_3 introduced by Roux and co-workers [29] is then clear and unambiguous.

The surface representing the membrane in L_3 then divides the 3D space in two and only two subvolumes which, although strongly interwoven, are totally disconnected from one another. Designating the two subvolumes at a given place as I and O, one actually generates an unambiguous labelling of the subvolumes everywhere in the sample (by the rule that each time a path goes through the bilayer, I is changed into O and conversely). This implies further that the sign of the unit vector normal to the surface is unambiguously defined everywhere, once it is specified arbitrarily at any given point on the bilayer. A characteristic feature of the bilayer is its symmetry with respect to a change of sign of its local normal. This local symmetry is expressed in the particular form of the bilayer elasticity (3'), which is necessarily invariant upon changing the signs of both c_1 and c_2. The labelling of the subvolumes I and O is therefore arbitrary, so that any Hamiltonian aiming to describe the system must be invariant under a global change of I and O. This exact local symmetry implies that the two subvolumes in L_3 should be, in general, statistically identical. But, it also raises the possibility that this global symmetry may be broken spontaneously for some appropriate conditions. In spite of its above-mentioned artificialities, a basic interest of the random-mixing model of section 4 is that it predicts such a spontaneous breaking of the global symmetry explicitly.

However, for the sake of generality, it is worthwhile avoiding a too strongly specified model. Following [29], we first define an order parameter η appropriately related to the degree of asymmetry of the phase. Such a choice is somewhat arbitrary and one could for instance take $\eta = 1/2 - \Psi$ where Ψ is the volume fraction of [I]: then we have $\overline{\eta} = 0$ in the symmetric case and $\overline{\eta} \neq 0$ in the asymmetric one. One can prefer an order parameter reflecting the average state of the membrane rather than that of the subvolumes [I] and [O]. A more appropriate choice should then be $\eta = (c_1 + c_2)\bar{d}$ since here again $\overline{\eta} = 0$ characterizes the symmetric state and $\overline{\eta} \neq 0$ the asymmetric one. Since our purpose is to build up an effective-Landau Hamiltonian, the specific choice of η is actually not of crucial importance. Considering now one situation with an average volume fraction of membrane $\overline{\phi}$ we define $\rho = \phi - \overline{\phi}$, which characterizes the local deviation from the mean concentration $\overline{\phi}$ of amphiphiles. The effective-Landau Hamiltonian involving the two order parameters ρ and η takes the form

$$H = \mu\rho + \lambda\rho^2 + \beta\eta^2 + \delta\eta^4 + \nu\rho\eta^2. \tag{39}$$

Since no particular symmetry is associated with ρ, odd powers of ρ are allowed (μ is here chosen such that $\overline{\rho} = 0$). In contrast, η has to reflect the exact symmetry of the membrane and only even powers of η are allowed. The most important consequence of the symmetry is that the term of lowest order in (39) which couples ρ and η is necessarily $\rho\eta^2$. This coupling term is quadratic in η and actually has a unique consequence on the light scattering pattern of L_3 samples. The intensity of the light scattered by the sample arises from the fluctuations of ρ but not directly from that of η. However, due to the coupling term $\nu\rho\eta^2$, fluctuations of η will affect the statistics of the ρ-fluctuations. In this sense, the scattering pattern will be

sensitive to η-fluctuations, but in an indirect way. To investigate this point we must use a Landau–Ginzburg Hamiltonian. The simplest way to do this is to add a gradient term for η : $\gamma(|\nabla\eta|^2)$ in (39). We neglect the gradient term for ρ consistently with the expectation that far from critical conditions the correlation length of ρ is small (basically of order $\bar{d}$). With this modification, the LG Hamiltonian can be written equivalently:

$$H_{LG} = \mu(\rho + \nu\eta^2/2\lambda) + \lambda(\rho + \nu\eta^2/2\lambda)^2 + (\beta - \mu\nu/2\lambda)\eta^2 + (\delta - \nu^2/4\lambda)\eta^4 + \gamma(|\nabla\eta|^2). \tag{40}$$

Having so diagonalized H_{LG}, it is clear that the internal variables $(\rho + \nu\eta^2/2\lambda)$ and η have independent fluctuations (no coupling term between them). Far from critical conditions, the η^4-term can be neglected and η simply shows gaussian fluctuations with a distribution controlled by $(\beta - \mu\nu/2\lambda)$. Thus, we simply expect

$$\langle\eta(0)\eta(r)\rangle = e^{-r/\xi_\eta}/4\pi\gamma r \tag{41}$$

where $\xi_\eta = \gamma/2(\beta - \mu\nu/2\lambda)$.

From (40) the local value of $\rho(r)$ has a gaussian probability distribution with variance $1/2\lambda$ around a mean value depending on the actual local value of $\eta(r)$:

$$(\mu - \nu\eta^2(r))/2\lambda. \tag{42}$$

Thus, we obtain for the density–density correlation function:

$$\langle\rho(0)\rho(r)\rangle = [\langle\eta(0)^2\eta(r)^2\rangle - \langle\eta^2\rangle^2]/\lambda^2 + \delta(r)/2\lambda. \tag{43}$$

Since the fluctuations of η are gaussian:

$$\langle\eta^2(0)\eta^2(r)\rangle = \langle\eta^2\rangle^2 + 2\langle\eta(0)\eta(r)\rangle^2 \tag{44}$$

we can write directly:

$$\langle\rho(0)\rho(r)\rangle = (1/\lambda^2)e^{-2r/\xi_\eta}/(4\pi\gamma r)^2 + \delta(r)/2\lambda. \tag{45}$$

The scattering pattern on a large scale ($q \ll 2\pi/d$) is simply obtained by Fourier transformation of (45) and it has the very unusual form:

$$I(q) = c_1[c_2 + \arctan(q\xi_\eta/2)/(q\xi_\eta/2)] \tag{46}$$

where c_1 and c_2 are related to λ, γ and ξ_η in a straightforward way. This form (equation (46)) is very different from the usual Ornstein–Zernicke q-dependence: at high q, the arctan term decays asymptotically as q^{-1} rather than q^{-2}. This unique dependence arises from the quadratic coupling between ρ and η in (39).

These ideas of a hidden symmetry in L_3 can therefore be checked unambiguously from classical light scattering measurements. An example of such data is shown in figure 13 where fits with the usual OZ-form and with (46) are given for the sake of comparison. Other very convincing experimental data are reported in [25] for other systems, supporting strongly the relevance of the η-fluctuations. Moreover, form (46) only applies for the symmetric case: in the asymmetric case where η fluctuates

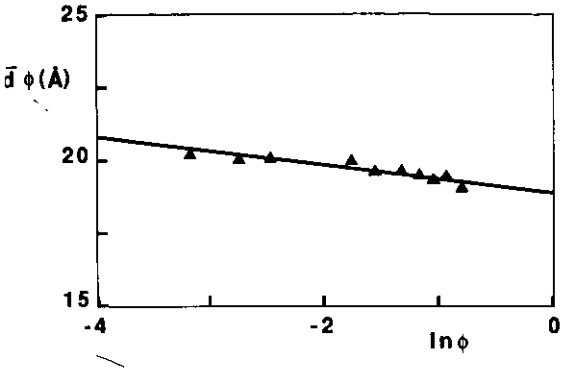

Figure 12. $\phi\bar{d}$ versus ln ϕ along a dilution line in L_α (from [25]). System: AOT/brine. From the slope, K_0 can be estimated according to [38]: K_0 is here of the order of $3k_BT$.

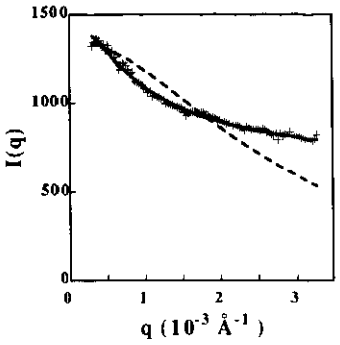

Figure 13. The low-q-scattering pattern of L_3 (light scattering). Broken curve, best fit with OZ; full curve: best fit with [46]. System: CP Cl/n-hexanol/brine.

around a finite mean value $\overline{\eta}$ the lower-order coupling term with ρ-fluctuations would be indeed linear (of the form $\rho(\eta-\overline{\eta})$) and a more conventional OZ-dependence of $I(q)$ would be expected. Thus, the above-mentioned data prove that L_3 is symmetric over large portions of its domain of stability.

Symmetric L_3 basically consists of one infinite bilayer. This structure is certainly not stable at extreme dilution: at some stage, the entropy of dispersion of disconnected pieces must overcompensate the cohesion energy of the infinite membrane. Keeping the picture of surfaces with no rims, we expect the membrane to survive in the form of a random distribution of closed vesicles, and the statistical symmetry between I and O subvolumes is no longer respected. Therefore, the symmetry in L_3 has to break at some point upon dilution. Much effort is currently being spent, in order to check whether the transition is continuous or not. Currently available data are in favour of a continuous transition [35], at least in some systems. Note however that form (46) for $I(q)$ is restricted to the case of gaussian statistics for η. This is obviously wrong close to the transition line. More detailed discussions of these interesting issues can be found in [36].

8. Conclusion

We have described how amphiphilic molecules can self-assemble into fluctuating 2D membranes, even in the dilute range. The phases so obtained actually provide exact experimental realizations of flexible random surfaces being confined in the limited volume of the samples. The statistics of these 2D objects is controlled by their bending elasticity. However, working out the corresponding statistical problem completely is actually out of our reach at the present time.

The two dilute phases of fluid membranes characterized here have very different structures on a large scale. The swollen lamellar phase L_α shows smectic order and the topology of the membranes is simply connected, just like that of planes. On the other hand, the anomalous isotropic phase L_3 shows no long-range order and the membranes are multiconnected over macroscopic distances along the three directions of space. Actually, the phase behaviour in the moderately dilute range can

be rationalized, at least qualitatively, in terms of the bending elasticity (K and $\overline{K}$) of the bilayers: K controls the curvature fluctuations, while $\overline{K}$ drives the topological transformations.

A remarkable property of the elastic Hamiltonian is its invariance with respect to dilation. This results, for the membranes' statistics, into a scale-invariance weakly broken by logarithmic renormalizations. This invariance rules the evolution of the physical properties of the phases upon dilution (scaling laws). The effects of the renormalizations are mild in the moderate dilution range but ultimately lead to a strong fluctuation regime at high dilution.

The striking persistence of the smectic order of the swollen lamellar phase can be understood in terms of the Helfrich steric interaction, arising from the constraint of non-intersection for nearby membranes. The $T^2K^{-1}d^{-2}$-dependence of the corresponding free-energy density per unit area of membranes is again derived from simple scaling arguments.

Finally, the exact local symmetry of the bilayer, with respect to changing the sign of its normal, implies the existence of a statistical global symmetry in the way it separates space in two disconnected subvolumes. The global symmetry of L_3 must break at some stage at high dilution. The quadratic coupling of the order parameter of the symmetry to the local concentration of membranes implies a very unusual q-dependence for the scattering factor of symmetric L_3 at low q. This remarkable feature is beautifully confirmed from light scattering experiments reported on various systems.

Some considerations on this last point must be stressed as an interesting further issue in this subject. In principle, the global symmetry described above only makes sense in the case of membranes totally free of 'holes'. But actually, the presence of a low density of small holes should not affect the situation too strongly: an ideal defect-free surface can be (mentally) drawn by continuity over such small defects: so the labelling of [I] and [O] remains uniquely defined. However, this is certainly no longer possible in a unique way if the average size of the holes becomes very large.

The excess energy associated with the formation of holes can be characterized by the line tension λ per unit length of edge on the membrane. At sufficiently high λ, holes are scarce and small and the symmetry remains well defined. Upon lowering λ below some critical value λ_c, the configurational entropy of large random loops compensates the energy cost due to the line tension: at λ_c, the average contour length of the edge loops diverges. This raises the possibility of a phase consisting of an infinite multiconnected membrane bearing infinite edges: Huse and Leibler call this phase the 'sponge with free edges' [37]. Of course, below λ_c subvolumes I and O can no longer be distinguished and the idea of global symmetry makes no sense.

Interestingly, the line tension λ is certainly related to c_0, the spontaneous curvature of the amphiphilic films: increasing c_0 decreases λ. So we guess that λ can be monitored experimentally by the same external parameters (salinity, composition of the bilayer) as those which have been shown to tune $\overline{K}$ (see section 3). Gathering these considerations on the symmetry [29] and on the line tension [37], together with the necessity that at extreme dilution everything must end up with disconnected vesicles and/or micelles, we expect phases of fluid membranes to exhibit very rich and unique behaviours in the high-dilution regime. We hope that experimental facts will soon be reported illustrating these expectations.

Acknowledgments

I would like to thank J Appell for many discussions and careful reading of the manuscript. The present description and interpretation of the L_α and L_3 phases progressively settled up along the long term collaboration I had with J Appell, P Bassereau and J Marignan. I also benefitted from illuminating discussions with D Roux and M E Cates.

References

[1] Ekwall P 1975 *Advances in Liquid Crystals* vol 1, ed G H Brown (New York: Academic) p 1
[2] Benton W J and Miller C A 1983 *J. Phys. Chem.* **87** 4981
[3] Huse D A and Leibler S 1988 *J. Physique* **49** 605
[4] Landau L and Lifshitz E (ed) 1980 *Course of Theoretical Physics: Statistical Physics* vol 5, 3rd edn (Oxford: Pergamon) p 396
[5] Helfrich W 1973 *Z. Naturf.* C **28** 693
[6] David F 1989 *Statistical Mechanics of Membranes and Surfaces* ed D Nelson, T Pvian and S Weinberg (New York: World Scientific) p 158
[7] Langevin D and Meunier J (ed) 1987 *Proc. Les Houches Workshop on Physics of Amphiphilic Layers* (Berlin: Springer)
[8] Larche F, Appell J, Porte G, Bassereau P and Marignan J 1986 *Phys. Rev. Lett.* **56** 1700
[9] Safinya C R, Roux D, Smith G S, Sinha S K, Dimon P, Clark N A and Bellocq A M 1986 *Phys. Rev. Lett.* **57** 2518
[10] Bassereau P, Marignan J and Porte G 1987 *J. Physique* **48** 673
[11] Roux D and Safinya C R 1988 *J. Physique* **49** 307
[12] Porte G, Marignan J, Bassereau P and May R 1988 *J. Physique* **49** 511
[13] Gazeau D, Bellocq A M, Roux D and Zemb T 1989 *Europhys. Lett.* **9** 447
[14] Porte G, Appell J, Bassereau P and Marignan J 1989 *J. Physique* **50** 1335
[15] Strey R, Schömacker R, Roux D, Nallet F and Olsson V 1990 *J. Chem. Soc. Faraday Trans.* **86** 2253
[16] Strey R, Jahn W, Porte G and Bassereau P 1990 *Langmuir* **6** 1635
[17] Porte G, Gomati R, El Haitami O, Appell J and Marignan J 1986 *J. Phys. Chem.* **90** 5746
[18] Sadoc J F and Charvolin J 1986 *J. Physique* **46** 683
[19] Petrov A G, Mitov M D and Derzhanski A 1978 *Phys. Lett.* **65A** 374
[20] Hendrickx Y, Charvolin J and Raviso M 1984 *J. Colloid Interface Sci.* **100** 597
Alperine S, Hendrickx Y and Charvolin J 1985 *J. Physique Lett.* **46** L27
[21] Helfrich W 1978 *Z. Naturf. a* **33** 305
[22] Cates M E, Roux D, Andelman D, Milner S T and Safran S A 1988 *Europhys. Lett.* **5** 733
[23] Golubovic L and Lubensky T C 1990 *Phys. Rev.* A **41** 4343
[24] Porte G, Delsanti M, Billard I, Skoouri M, Appell J, Marignan J and Debeauvais F 1991 *J. Physique* II **1** 1101
[25] Skouri M, Marignan J, Appell J and Porte G 1991 *J. Physique* II **1** 1121
[26] Helfrich W 1985 *J. Physique* **46** 1263; 1987 *J. Physique* **48** 285
[27] Peliti L and Leibler S 1985 *Phys. Rev. Lett.* **54** 1690
[28] David F 1988 *Europhys. Lett.* **6** 6083
[29] Roux D, Cates M E, Olsson U, Ball R, Nallet F and Bellocq A M 1990 *Europhys. Lett.* **11** 229
[30] de Gennes P G and Taupin C 1982 *J. Phys. Chem.* **86** 2294
[31] Caillé A 1972 *C.R. Acad. Sci.* B **274** 891
[32] Gunther L, Imry Y and Lajzerowicz J 1980 *Phys. Rev.* A **22** 1733
[33] Roux D, Nallet F, Freyssingeas E, Porte G, Bassereau P, Skouri M and Marignan J 1992 *Europhys. Lett.* **17** 575
[34] Appell J, Bassereau P, Marignan J and Porte G 1990 *Progr. Colloid Polym. Sci.* **81** 13
[35] Coulon C, Roux D and Bellocq A M 1991 *Phys. Rev. Lett.* **66** 1709
[36] Pfeuty P 1991 Comment on [35] and *Physica* A **177** 197
[37] Huse D A and Leibler S 1991 *Phys. Rev. Lett.* **66** 437